Trivelpiece-Gould modes in a corrugated plasma slab

A. M. Ignatov
General Physics Institute, 38 Vavilova St., Moscow, Russia
(Received 21 July 1994)

It is shown that the spectrum of electrostatic oscillations in a periodically corrugated plasma slab exhibits spatial mode locking, i.e., for each spectral branch there is an infinity of subbands with constant wave numbers. The widths of the largest subbands are evaluated. We also show that the eigenmodes are represented by a set of double layers. Under certain conditions, the initial problem for wave propagation is solved. The interaction of an electron beam with a plasma is studied and the corresponding instability growth rate is obtained.

PACS number(s): 52.25.Wz

I. INTRODUCTION

A. Overview

Although many theoretical studies on the wave propagation deal with unbounded media, both natural and laboratory plasmas are confined by some external fields or walls. There are usually no severe troubles with boundaries of relatively simple shape and properties. For example, confining a magnetized homogeneous plasma by the perfectly conducting cylindrical wall results in quantization of the transverse wave number, i.e., the appearance of a set of the well-known Trivelpiece-Gould (TG) modes [2]. However, in looking for the ways to improve various plasma devices, the fancy of designers goes beyond this simple example and the necessity of studying waves in resonators of more complicated shapes is topical.

Recently, it has been shown that generators of coherent electromagnetic radiation employing plasma-filled spatially periodic retarding structures have some beneficial features (see, e.g., [1] and references therein). Of particular interest is the introduction of plasma into a corrugated waveguide in order to get better conversion of electron beam energy to electromagnetic radiation. In studying the wave propagation in such a device, it was unexpectedly observed that the wave spectrum exhibits extremely odd behavior [1].

It turned out that instead of being a set of curves like TG modes the spectral dependence looks like an infinitesimally fine grid filling the entire frequency band between zero and the plasma frequency. Since this grid constitutes a dense set, the corresponding wave spectrum was called a dense one. In other words, this means that any frequency is either a solution to the dispersion relation or is infinitesimally close to a solution.

In the present paper, we investigate various aspects of this phenomenon in a magnetized plasma slab depicted schematically in Fig. 1. In application to this case, the reasoning of the paper [1] may be reproduced as follows. The wave spectrum in a smooth plasma slab consists of a set of TG modes [2]:

$$\Omega_n(k) = \frac{k\omega_p}{\sqrt{q_n^2 + k^2}} , \tag{1}$$

where we assume that the slab is immersed in a strong magnetic field ($B_z \to \infty$). Here, k is the longitudinal wave number, ω_p is the plasma frequency and, with $2a_0$ being the slab thickness, $q_n = \pi(n + 1/2)/a_0$ for the even eigenmodes or $q_n = \pi n/a_0$ for the odd eigenmodes, respectively.

Suppose now that the conducting surface surrounding the plasma is periodically corrugated as shown in Fig. 1, and the corrugation amplitude is sufficiently small. Operating according to standard perturbation theory prescriptions, to obtain the spectrum of a spatially periodic structure, one must draw in the (ω, k) plane an infinity

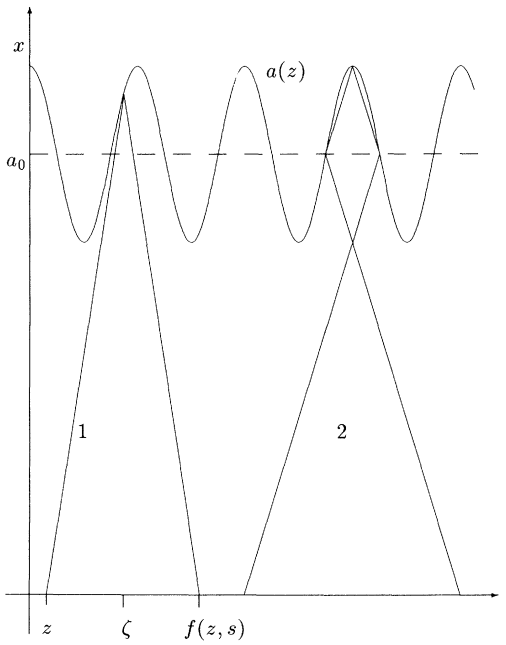

FIG. 1. Schematic diagram of a corrugated plasma slab. Perfectly conducting walls confining a magnetized plasma are at $x = \pm a(z)$. The wave fronts 1, 2 are constructed of straight-line segments with $\Delta x = \pm s\Delta z$. The curve 1 shows the way the circle map $f(z, s)$ is constructed. The curve 2 corresponds to the multiple reflections of the wave front ($s < s_{\min}$) which cannot be described by a circle map.

of unperturbed curves (1) shifted by $k_0 = 2\pi/L$ along the k axis, where L is the period of perturbation (see Fig. 2, where a few first iterations for even eigenmodes are shown). All TG modes are confined to a finite frequency band and each unperturbed curve intersects with an infinity of shifted curves with some coupling at the intersection points resulting in small frequency gaps at intersection points. For simplicity, these gaps are not shown in Fig. 2. It may be easily shown that the obtained grid fills densely a finite area in the (ω, k) plane.

There are few problems springing about dense spectra. First, drawing the pictures like Fig. 2, one should use either the extended or the reduced Brillouin zones [3]. For example, unlike solid state physics where the similar problem arises, it is not evident how the described grid reduces to the unperturbed spectrum (1) as periodic corrugation tends to zero. Formally, in this limit the dense spectrum remains dense, while we would like to get usual TG modes. Seemingly, this indicates that the graphic representation of the spectrum (Fig. 2) contains some spurious information.

On the other hand, a similar problem was discussed by Gusakov and Piliya [4]. They used the geometric-optics approximation to study a hybrid resonance in a periodically inhomogeneous waveguide and revealed that there exists a single ray path attracting all other paths. This means that the corresponding eigenmodes are singular functions and, therefore, even for a small perturbation, high-order spatial harmonics are relevant. Thus, another problem is whether the straightforward perturbational approach using a few harmonics is valid.

In the present paper, some exact analytical results concerning the wave spectra in a corrugated plasma slab are obtained. Our main finding is that one can extract single wave branches analogous to the TG modes from the grid depicted in Fig. 2 or, in other words, the appropriate spectral classification is found. It is shown that for any wave branch the spectral dependence exhibits the spatial mode locking, i.e., the entire frequency range is split in an infinite number of subbands and the wave number is constant in each of these subbands. The spectrum of this kind is represented by a fractal curve that was named a devil's staircase [5]. We evaluate the width and the position of the largest subband for an arbitrary waveguide boundary, $a(z)$, smaller subbands are studied by numeric methods. The spatial structure of the eigenmodes is shown to correspond to a quasiperiodic set of double layers, i.e., a sequence of the electric field pulses. Finally, we study the excitation of these waves by an electron beam and evaluate the growth rate of the corresponding instability.

This paper is organized as follows. Since we use the mathematical theory of the so-called circle maps a brief review of the formalism is given in the next subsection. In Sec. II, we present the mathematical formulation of the problem, demonstrate how it is reduced to investigation of circle maps and evaluate some characteristics of the spectrum. Section III deals with the spatial structure of waves and, in Sec. IV, the temporal evolution of a waveform is discussed. In Sec. V, we consider the interaction of plasma waves with an electron beam. Some concluding remarks are made in Sec. VI. Appendix A contains general expressions for eigenfunctions. The numeric methods we used are described in Appendix B.

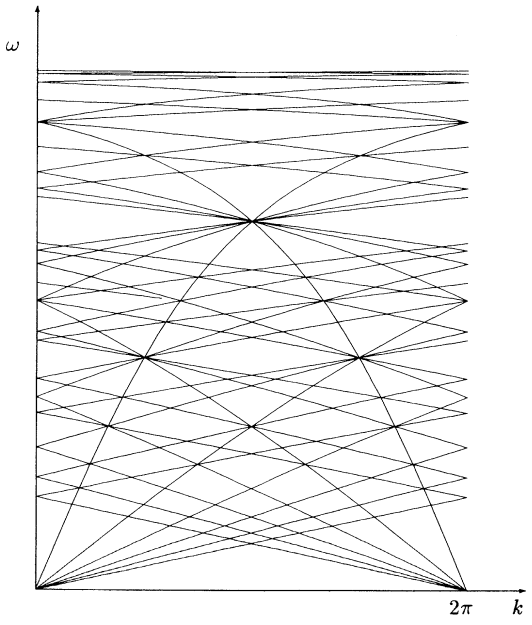

FIG. 2. Dense spectrum in a planar waveguide. The grid is composed of the original TG modes (those coming through the origin) shifted by $2\pi n$ along the k axis.

B. Circle maps

The theory of circle maps has a number of applications in physics, particularly, in studying the transition to chaos [5, 6]. Generally, a circle map is just a function $f(z)$ of a single variable z, such that

$$f(z+1) = f(z) + 1 \ . \tag{2}$$

Of importance for our purposes are the serial iterations of the circle map, which are characterized by the winding number, i.e., the mean number of rotations per iteration, defined through

$$W = \lim_{n\to\infty} \frac{z_n - z_0}{n} \ , \tag{3}$$

where $z_n = f^{(n)}(z_0)$ stands for the nth iteration of the map. A number of solid theorems hold for circle maps [7]; we will need the following statements, which are valid if $f(z)$ is smooth and invertible [i.e., $f'(z) > 0$]. The limit in Eq. (3) exists and is independent of the initial point, z_0. The asymptotic behavior of the series composed of successive iterations z_n depends essentially on the winding number. If it is a rational fraction, $W = P/Q$, where P and Q are some integers, then z_n converges to a periodic cycle, i.e, asymptotically $z_{n+Q} = z_n + P$. With irrational W, the series is quasiperiodic, that is, $\{z_n\}$ fills ergodically the whole interval (0,1), where $\{z\}$ denotes

the fraction part of a real number.

Of great interest is the dependence of the winding number on additional parameters. Suppose that the circle map depends on some other variable s, i.e., $f = f(z, s)$. Then the dependence $W(s)$ exhibits a phenomenon called the mode locking: if $W(s) = P/Q$ is rational then it remains constant with s varying in some interval. The last property may be understood in a following way. Suppose, there is a root of the equation $f^{(Q)}(z_0, s) = z_0 + P$, then according to Eq. (3) the winding number is rational. Other cycle elements satisfy the same equation and may be obtained by serial iterations of the map: $z_i = f^{(i)}(z_0, s), i = 1, \ldots, Q-1$. Obviously, if $f(z, s)$ is a continuous function, then small variations of s cannot change the number of roots and, therefore, $W(s)$ is constant. $W(s)$ is an example of the so-called devil's staircase, i.e., a continuous function that remains constant in some interval when its value is a rational number.

Thus the domain of definition of $W(s)$ contains an infinite number of mode-locked intervals distinguished by rational values of $W(s)$. The question of importance is how much room all mode-locked intervals take. There is a general statement: if $f(z, s)$ differs slightly from the linear function, $f(z, s) = z + \epsilon\Delta f(z, s)$, then the Lebesque measure of the mode-locked intervals is small if $\epsilon \to 0$, i.e., the probability of finding the rational wave number for a randomly chosen value of s is nearly zero [7].

II. CIRCLE MAPS AND PLASMA OSCILLATIONS

A. Basic equations

We start with the Poisson equation

$$\frac{\partial^2\phi}{\partial z^2} - s^2\frac{\partial^2\phi}{\partial x^2} = 0 \tag{4}$$

for the amplitude of electrostatic oscillations, $\phi(x, z)$, with frequency ω [i.e., the time-dependent potential is $\mathrm{Re}(\phi e^{-i\omega t})$], where $s^2 = -1/\epsilon(\omega) = \omega^2/(\omega_p^2 - \omega^2)$. This equation was derived in assumption that the magnetic field is strong enough to neglect the transverse particle motion and the unperturbed plasma is uniform. In the frequency range, we are interested in $\omega_p^2 > \omega^2$, i.e., $s^2 > 0$, the equation (4) is of hyperbolic type.

Since we consider a plasmaguide confined by symmetric perfectly conducting walls (Fig. 1), the first boundary condition for Eq. (4) is

$$\phi(\pm a(z), z) = 0, \tag{5}$$

where $a(z)$ is some periodic function. Henceforth, we choose the spatial scale so that the period is unity, $a(z+1) = a(z)$. The wave number, k, is introduced by the second boundary condition,

$$\phi(x, z+1) = e^{ik}\phi(x, z). \tag{6}$$

Here we use the extended Brillouin zones, so that k is any real number.

Equations (4)–(6) represent the mathematical formulation of the problem we are studying. Certainly, besides plasma physics, Eq. (4) has a great number of other applications, and much work has already been done. Seemingly, for the first time its exact solution for an arbitrary boundary $a(z)$ was found in application to the supersonic flows in the 1950's with the help of the h-conformal mappings[8]. If we consider z in Eq. (4) as a time variable, then it describes a wave field (e.g., sound or light) in a resonator with moving walls [9, 10]: an interesting problem under intensive investigation. However, there is one feature distinguishing the problem of plasma wave propagation: in most other applications s in Eq. (4) is some constant, while here it is a spectral parameter and what we are looking for is the dependence $s(k)$ or vice versa.

The general solution of Eqs. (4) and (5) is constructed in the following way [8]. Due to the mirror symmetry of a plasmaguide, any eigenmode must be either odd or even in x. Thus, generally, the potential looks like

$$\phi(x, z) = A(z + x/s) - (-1)^\lambda A(z - x/s), \tag{7}$$

where λ is 0 or 1 for odd and even modes, respectively, and $A(z)$ is an arbitrary function. Substituting this solution into the boundary condition (5) results in

$$A(z + a(z)/s) = (-1)^\lambda A(z - a(z)/s). \tag{8}$$

Let us suppose that s is large enough, $s > s_{\min} = \max|a'(z)|$, therefore we restrict the discussion to a certain frequency range, $\omega_{\min} < \omega < \omega_p$, where $\omega_{\min} = \omega_p s_{\min}/\sqrt{1 + s_{\min}^2}$. Next, we introduce a function, $f(z, s)$, defined parametrically as

$$z = \zeta - a(\zeta)/s,\ f(z, s) = \zeta + a(\zeta)/s,\ -\infty < \zeta < \infty \tag{9}$$

(see Fig. 1, the line 1). The imposed constraint, $s > s_{\min}$, means that a characteristic curve leaving the z axis is reflected only once before it turns back, i.e., here we do not consider the situation shown by the line 2 in Fig. 1. Obviously, $\partial f(z, s)/\partial z > 0$ and if $a(z)$ is periodic then $f(z+1, s) = f(z, s) + 1$, so $f(z, s)$ is a circle map.

Rewriting Eq. (8) as $A(f(z, s)) = (-1)^\lambda A(z)$, we seek the solution in the form of

$$A(z) = \exp[i\pi(2n + \lambda)\psi(z)], \tag{10}$$

where n is an arbitrary integer, $\lambda = 0, 1$ and the phase, $\psi(z)$, obeys the relation

$$\psi(f(z, s)) - \psi(z) = 1\ , \tag{11}$$

which may be resolved in the following way. Let us consider an interval $I_0 = (z_0, z_1)$, where $z_1 = f(z_0, s)$ and z_0 is an arbitrary number. Since $f(z, s)$ is monotonic, each point z may be linked with another point $z' \in I_0$ by a number of iterations, i.e., $z = f^{(m)}(z', s)$. Thus, according to Eq. (11), the phase $\psi(z)$ is determined by its value in the interval I_0: $\psi(z) = \psi_0(f^{(-m)}(z)) + m$, where $\psi_0(z)$ is an arbitrary function such that $\psi_0(z_1) = \psi_0(z_0) + 1$ and its derivatives of up to the desired order are equivalent at the points $z_{0,1}$.

It should be noted that there is an infinite set of eigenmodes distinguished by different n's in Eq. (10). Therefore, even without implementing the periodicity condition (6), we conclude that the spectrum of oscillations may be split quite naturally in different spectral components and, in fact, Fig. 2 or, rather, its limit image shows the superposition of an infinity of different graphs.

In terms of the phase, the periodicity boundary condition (6) is

$$\psi(z+1) = \psi(z) + \kappa, \tag{12}$$

where $k = \kappa\pi(2n+\lambda)$, i.e., the spectra of all wave modes are determined by a single function $\kappa(s)$. To obtain it, one must find $\psi(z)$ and corresponding $\kappa(s)$ satisfying both relations (11) and (12), while the described above solution generally does not obey Eq. (12): this is the problem we focus on throughout the paper.

Let us consider the familiar example of a smooth plasmaguide. In this case, $a(z)$ is a constant and $f(z,s) = z + 2a/s$, therefore

$$\psi(z) = \kappa z,\ \kappa(s) = s/2a \tag{13}$$

which, as one can easily verify, corresponds to the usual TG modes. These relations will be a checkpoint for any solution of the set (11,12): there must be some transition to expressions (13) as $a(z)$ tends to a constant.

B. Winding number and wave number

Suppose that the winding number is rational and there is the Q/P cycle, i.e., a sequence $\alpha_0, \alpha_1, \ldots, \alpha_{Q-1}$ such that $\alpha_i = f(\alpha_{i-1}, s)$ and $f(\alpha_{Q-1}, s) = \alpha_Q = \alpha_0 + P$. We simplify the problem restricting the discussion to the class of functions $a(z)$, such that there is only one minimum and one maximum over the period. Then, for each s, there are two cycles, called stable and unstable ones distinguished by the $\pm$ superscript. The difference between them is in asymptotic behavior of the sequence $\theta_n = \{f^{(nQ)}(z)\}$: $\theta_n \to \alpha_0^-$ as $n \to \infty$, and $\theta_n \to \alpha_0^+$ as $n \to -\infty$.

The relation between the winding number of the map $f(z,s)$ and the wave number κ is fairly evident. Making use of Eqs. (11) and (12), we get

$$\psi(z_Q, s) = \psi(z_0, s) + Q = \psi(z_0) + P\kappa, \tag{14}$$

therefore,

$$\kappa = \frac{Q}{P} = \frac{1}{W(s)}\ . \tag{15}$$

Since any irrational number may be approximated by a rational number, we may conclude that the relation (15) holds even for the irrational winding number.

As we have already mentioned, the dependence of the winding number, and therefore, the wave number on s performs the devil's staircase consisting of an infinite number of plateaus. Let us denote the plateau corresponding to a Q/P cycle as $\Delta_{Q/P}$. Since s is nothing but the renormalized frequency, we conclude that the spectral curve $\omega(\kappa)$ looks extremely odd, at least for plasma physics: it is nondifferentiable dependence consisting of a set of vertical lines for each rational κ. In other words, what we face is the spatial mode locking: the entire frequency band is split in a number of subbands with constant wave numbers.

Suppose now that the waveguide is nearly smooth, i.e., let the deviation of $a(z)$ from the constant be of the order of $\epsilon \ll 1$. Then it may be easily shown that the dependence $\kappa(s) = s/2a_0 + \Delta\kappa$, where a_0 is the average width of a waveguide, and for any Q/P cycle $\Delta\kappa \le \epsilon^Q$ [7]. In this sense, there is the limiting transition to the usual TG modes: although $\kappa(s)$ remains irregular for $\epsilon \neq 0$, it tends to the first expression in Eqs. (13) as $\epsilon \to 0$.

C. $Q = 1$ plateaus

The width of a plateau with $Q = 1$ can be easily evaluated. Taking into account Eq. (9), we rewrite the relation $f(z,s) = z + P$ as

$$s = \frac{2}{P} a\left(z + \frac{P}{2}\right) = \sigma(z), \tag{16}$$

which implicitly defines the cycle points of the map: there are two roots of this equation, $z = \alpha_0^{(\pm)}$, distinguished by the sign of the derivative, $\sigma'(\alpha_0^-) < 0$, $\sigma'(\alpha_0^+) > 0$. Equation (16) also defines the interval of s in which the cycle with $Q = 1$ exists, i.e., we obtain the fundamental set of plateaus corresponding to the lowest resonance,

$$\Delta_{1/P} = \left[\frac{2}{P} a_{\min},\ \frac{2}{P} a_{\max}\right], \tag{17}$$

where $a_{\min}$ and $a_{\max}$ stand for minimum and maximum values of $a(z)$, respectively.

D. Numerical evaluation

We performed a series of computer runs to evaluate the parameters of other plateaus using the cosine-shaped boundary

$$a(z) = \frac{1}{2} + \frac{\epsilon}{2\pi}\cos(2\pi z). \tag{18}$$

The implemented algorithm is described in Appendix B. For the specific shape (18), one can easily check that the plateaus with $Q = 2$ are of zero width. In comparison to the previous studies of a devil's staircase, e.g., [6], the computations with the implicitly defined circle map (9) are a much more computer-time consuming task, which is why we were able to proceed up to $Q = 100$ only. However, this seems pretty enough for any physical application because of the exponential reduction of the plateau width.

In Fig. 3, which shows an example of the dependence $\kappa(s)$ evaluated for $\epsilon = 0.1$, only the largest plateau, $\Delta_{1/1}$, is visible, while all high-order resonances results in negligible plateaus. With increasing ϵ, the width of the plateaus grows but, on the other hand, the range of

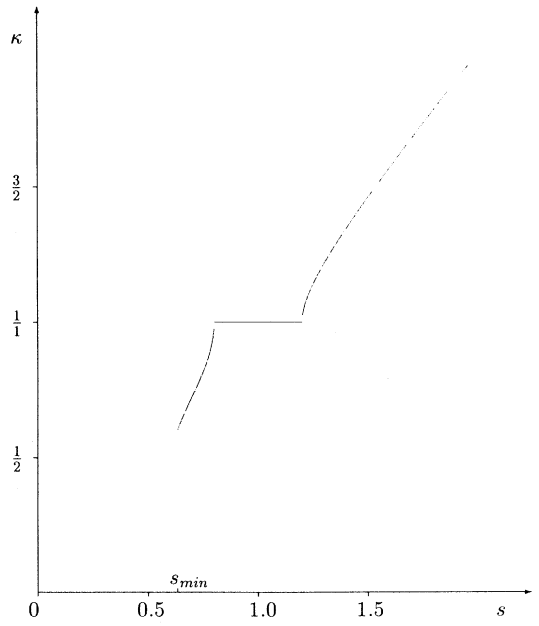

FIG. 3. Dependence of the wave number on s, $\epsilon = 0.1$. The devil's staircase consists of a set of plateaus for each rational κ. Here, the only visible plateau corresponds to $\kappa = 1/1$.

validity of the present theory moves up the s axis. In Fig. 4 depicted for $\epsilon = 0.2$, the left edge of the fundamental plateau, $\Delta_{1/1}$, hits the forbidden area, $s < s_{\min}$. The self-similar structure of the devil's staircase is clearly visible in the magnified part of this curve also shown in Fig. 4. It is noteworthy that $\kappa(s)$ tends to the unperturbed dependence (13) at large s.

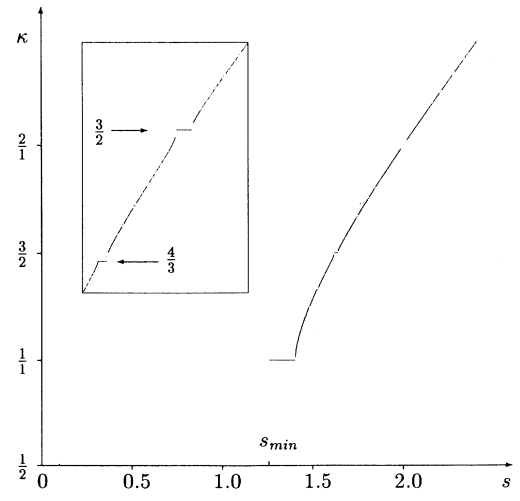

FIG. 4. Dependence of the wave number on s, $\epsilon = 0.2$. With increasing wall corrugation, ϵ, the widths of plateaus grow. The magnified part of the curve shows its self-similar structure.

III. SPATIAL STRUCTURE OF A WAVE

A. Eigenfunctions

Our purpose, in this section, is to make out the spatial structure of the TG waves. Let us consider what happens to Eq. (11) under the successive iterations of the map $f(z,s)$. For simplicity, we focus on fundamental plateaus with $Q = 1$; more bulky expressions concerning arbitrary cycles may be found in Appendix A. Now there is only one stable, α_0^+, and one unstable, α_0^-, cycle element per unit interval. Since $\{f^{(n)}(z)\}_{n\to\infty} \to \alpha_0^-$, it follows from Eq. (11) that

$$\{\psi(z)\} = \{\psi(f^{(n)}(z))\}_{n\to\infty} \to \{\psi(\alpha_0^-)\} \,. \tag{19}$$

The only points for which this relation fails are the unstable cycle points $\alpha_0^+ + n, n = 0, \pm 1, \ldots$. Therefore, $\psi(z)$ is a stepwise constant function with discontinuities at unstable cycle points. Evidently, the periodicity condition (12) is satisfied only if the height of each step is $1/P$.

Replacing $n \to -n$, $\alpha_0^- \to \alpha_0^+$ in Eq. (19) results in the second solution of the set (11),(12) in the form of the same function with discontinuities at the stable cycle points, hence, there are two independent solutions. Moreover, one can easily guess that the solution for an arbitrary $Q \neq 1$ is constructed in the same way: the only difference is that there are Q cycle elements, and, respectively, Q steps per unit interval, $1/P$ height each. As it was already mentioned, with small plasmaguide corrugation when $f(z,s)$ is close to a linear function, the winding number is irrational for nearly all values of s. The irrational winding number is a limit $Q \to \infty, P \to \infty, P/Q = \text{const}$, thus there are more and more steps of decreasing height per unit interval as the waveguide corrugation goes to zero for most values of s and the phase $\psi(z)$ becomes a smooth function — in this sense, the transition to the unperturbed planar plasmaguide (13) should be understood.

Coming back to the fundamental plateaus with $Q = 1$, we can easily write down the expression for the derivative of $A(z)$ (10), i.e., for the z component of the electric field at the axis:

$$A_z'^{\eta}(z,s) = \sum_{m=-\infty}^{\infty} e^{\frac{\pi i m}{P}} \delta\left(z - \alpha_0^{\eta}(s) - m\right), \tag{20}$$

where to reduce the notation, we have chosen the lowest even eigenmode in Eq. (10), i.e., $n = 0, \lambda = 1$. Since there are two independent eigenfunctions for each s, they are distinguished by the superscript $\eta = \pm 1$.

Thus, we see that the electric field of a TG wave in a certain frequency range is nonzero along the polygonal line 1 in Fig. 1, prolonged periodically to the whole slab. The spatial Fourier transform of the highly singular distribution (20) corresponding to the infinite periodic set of double layers is readily performed — obviously, all spatial harmonics are of the same amplitude and no straightforward perturbational expansion can result in a solution of this kind.

B. Completeness of the set of eigenfunctions

The next problem to study is whether we are able to use the functions (20) as a basis for expansion. Let us denote one of the intervals for which $\sigma'(z) > 0$, say, closest to zero, as M^+ and let the adjacent interval where $\sigma'(z) < 0$ be M^-. Evidently, the total length of both intervals is unity. Evaluating the integral

$$I^\eta(z) = \int_{\Delta_{1/P}} ds A_z'^\eta(z,s) F'(s) \ , \tag{21}$$

performed over the whole $Q = 1$ plateau, where $F(s)$ is an arbitrary function, results in

$$I^\eta(z) = \begin{cases} \eta \frac{dF(\sigma(z))}{dz}, & z \in M^\eta \\ 0, & z \notin M^\eta \end{cases} \tag{22}$$

and

$$I^\eta(z+1) = e^{\pi i/P} I^\eta(z). \tag{23}$$

Combining Eqs. (21)–(23), we can write down the representation for an arbitrary function, $f(z)$, obeying the condition (23) in the form of the Stieltjes integral

$$f(z) = \sum_{\eta=\pm} \eta \int_{\Delta_{1/P}} ds A^\eta(z,s) \tilde{f}'^\eta(s), \tag{24}$$

where

$$\tilde{f}^\eta(s) = f(\alpha_0^\eta(s)). \tag{25}$$

Thus, we see that eigenfunctions of the corrugated plasmaguide in a certain frequency range form a complete set in a class of periodic functions (23). Similar expressions may be obtained for a cycle with $Q \neq 1$, but besides periodicity some additional constraints on $f(z)$ must hold (Appendix A).

IV. TEMPORAL EVOLUTION OF A WAVE FORM

Until now, our main finding was the odd spectral dependence, $\omega(k)$, represented by a fractal curve consisting of an infinity of vertical lines. However, of greater importance for physics is the evolution of a wave form consisting of many temporal harmonics. Obviously, since the spectral curve is nondifferentiable, we are no longer able to use such concepts as group velocity and dispersion in application to the spectrum of this kind.

Nevertheless, using the results of Sec. III, we can easily solve the initial problem for the wave form. Suppose that initially, say, at $t = 0$, the quasiperiodic perturbation complying with Eq. (23) was excited. Then, making use of the transform (24), (25) and taking into account that each s component of the potential $\tilde{\phi}^\eta(s)$ oscillates with its own frequency $\omega(s)$, we easily obtain the expression for the z component of the electric field at the axis,

$$E_z(z,t) = \mathrm{Re} e^{-i\Omega(z)t} E_{0z}(z), \tag{26}$$

where E_{0z} is the initial electric field and $\Omega(z) = \omega(\sigma(z))$. This solution is quite natural because we have imposed the periodicity condition, i.e., all spectral components of the wave form are in the single plateau of the devil's staircase with the same P and $Q = 1$. Consider now the narrow spectral line of width $\Delta\omega$ with the maximum at $\omega = \omega_0$, then the electric field of the corresponding wave form looks like a double layer of finite width $\Delta\omega/\Omega'(z_0)$ intersecting the axis near one of the points z_0, such that $\Omega(z_0) = \omega_0$. Although the electric field of the form is still governed by Eq. (26), the amplitude of the spatially averaged field decays as $\exp(-\Delta\omega^2 t^2)$. This decay provided by the phase mixing between various modes is well known in isotropic plasmas with continuous spectrum (e.g., [11]). The initial electric field may be smooth, but very soon there appear large gradients yielding the Landau damping, that is, another phase mixing.

With the wave form overlapping at least two plateaus of the devil's staircase, it contains an infinite number of smaller plateaus and the corresponding expression for the temporal evolution turns out to be extremely bulky and a little informative. However, the behavior remains qualitatively the same. The temporal scale of the phase mixing is determined by the largest plateau width and by the phase relations between various plateaus. With the wall corrugation tending to zero, there should be uniform motion of the wave form afflicted by dispersion spread, but an attempt to trace this reduction failed.

V. BEAM-PLASMA INTERACTION

A. Basic equations

In this section, we consider the excitation of the described plasma waves by an electron beam. Suppose that the beam is of the form of an infinitesimally thin sheet at the $x = 0$ plane and propagates along the external magnetic field. Instead of the Poisson equation (4), we now have

$$\frac{\partial^2\phi(x,z)}{\partial z^2} - [s(\omega)]^2 \frac{\partial^2\phi(x,z)}{\partial x^2} = 4\pi e [s(\omega)]^2 \lambda(z)\delta(x), \tag{27}$$

where $\lambda(z)$ is the deviation of the surface beam density from its equilibrium value, λ_0, and the frequency, ω, is generally a complex quantity. It should be noted that within the present approach, it does not matter whether the beam space charge is neutralized. Using the continuity equation and the equation of motion for beam electrons, we get

$$\left(-i\omega + u\frac{\partial}{\partial z}\right)^2 \lambda(z) = \lambda_0 \frac{e}{m} \left.\frac{\partial^2\phi}{\partial z^2}\right|_{x=0}, \tag{28}$$

where u is the initial beam velocity.

Due to the mirror symmetry of the slab, even plasma modes only can interact with the beam, i.e, the solution of Eq. (27) is

$$\phi(x,z) = \begin{cases} F(z + x/s(\omega)) + G(z - x/s(\omega)), & x > 0 \\ F(z - x/s(\omega)) + G(z + x/s(\omega)), & x < 0 \end{cases}. \tag{29}$$

Finally, making use of the boundary conditions for the potential at $x = 0$ and $x = a(z)$ and taking into account Eq. (28), we obtain the desired set of equations describing beam-plasma interaction,

$$F(z) - G(z) = \nu(z) , \tag{30}$$

$$F(z + a(z)/s(\omega)) + G(z - a(z)/s(\omega)) = 0 ,$$

$$\left(-i\omega + u\frac{\partial}{\partial z}\right)^2 \nu(z) = -s(\omega) g_0 [F'(z) + G'(z)] , \tag{31}$$

where $\nu'(z) = -2\pi e s(\omega)\lambda(z)$ and the acceleration $g_0 = 2\pi e^2 \lambda_0/m$ is a two-dimensional analog of the plasma frequency.

The general solution of Eqs. (30) and (31) requires the analysis of a circle map in a complex plane that seems too complicated to be studied analytically. However, with a rarefied beam, we expect the spatial distribution of the electric field to be slightly altered by the beam and use the expansion in powers of the beam density. Thus, the problem is split into two parts: the first one is the approximate solution of the functional equations (30) providing the plasma response to the beam charge and the second task is to solve Eq. (31) which eventually should result in the growth rate of the beam-plasma instability.

B. Plasma response

Assuming that the beam line, $\omega = ku$, intersects one of the fundamental plateaus, $\Delta_{1/P}$ at the frequency $\omega_0 = \pi u/P = k_0 u$, we look for the solution with the frequency close to ω_0 satisfying the relation (23). To solve the first part of the problem let us apply the integral transform (24), (25) to Eqs. (30), i.e., represent, for example, $F(z)$ as a superposition of a set of double layers:

$$F(z) = \sum_{\eta=\pm} \eta \int_{\Delta_{1/P}} ds' A^\eta(z,s') \tilde{F}'^\eta(s'), \tag{32}$$

where s' is an auxiliary real parameter, that results in

$$\tilde{F}^\eta(s') - \eta F\left(f(\alpha^\eta(s'), s(\omega))\right) = \tilde{\nu}^\eta(s'). \tag{33}$$

Assuming that $\tilde{F}^\eta(s')$ is nonzero in the nearest vicinity of $s_0 = s(\omega_0)$, expanding Eq. (33) in powers of $[s(\omega) - s']$ and performing the transform (24), we obtain after some algebra

$$F'(z) = -\frac{1}{2}\mu(z)\frac{\nu(z)}{s(\omega) - \sigma(z)}, \tag{34}$$

where

$$\mu(z) = \frac{2}{P}\sigma(z) - \sigma'(z) \tag{35}$$

is a positive periodic function. Thus, the plasma response to the external perturbation generally results in the excitation of a set of sharp electric field spikes situated near the zeros of the denominator in Eq. (34).

C. Beam-plasma instability

Since we expect that the beam-plasma interaction is efficient only near the singularities, one can neglect the difference between $F(z)$ and $G(z)$ in Eq. (31), which may now be written as

$$\left(-i\omega + u\frac{\partial}{\partial z}\right)^2 \nu(z) = \frac{s g_0 \mu(z)}{s - \sigma(z)}\nu(z). \tag{36}$$

The latter should be supplemented with the periodicity condition (23). Equation (36) looks like the Rayleigh equation [12] for incompressible fluid and may be solved in the same way.

First, we note that the zeros of the denominator at $\mathrm{Im} s = 0$ in Eq. (36) result in logarithmic singularities of $\nu(z)$ proportional to $[z - \alpha^\pm(s)]\ln[z - \alpha^\pm(s)]$. Following the standard procedure [12] for the Rayleigh equation, we conclude that $\nu(z)$ is a continuous function, while its derivative at the singular points is discontinuous:

$$\nu'(\alpha^\pm + 0) - \nu'(\alpha^\pm - 0) = -i\pi s g_0 \frac{\mu(\alpha^\pm)}{|\sigma'(\alpha^\pm)|}\nu(\alpha^\pm), \tag{37}$$

where the choice of the sign in the right-hand side guarantees that the solution is analytic in the upper half of the complex ω plane.

Keeping the lowest order terms of expansion in powers of the beam density, i.e., g_0, far away from singular points in Eq. (36), one can set $g_0 = 0$, resulting in $\nu(z) = \exp(i\frac{\omega}{u}t)(C_1 + C_2 z)$, where $C_{1,2}$ are constants. Finally, taking into account that there are two singular points over the period and making use of Eqs. (23) and (37), we obtain the desired dispersion relation for the beam-plasma instability,

$$(\omega - \omega_0)^2 = i\frac{\pi}{2} s_0 g_0 \sum_{\eta=\pm} \frac{\mu(\alpha^\eta)}{|\sigma'(\alpha^\eta)|}, \tag{38}$$

therefore, the growth rate, γ, is

$$\gamma = M_1\sqrt{g_0 k_0}, \tag{39}$$

where M_1 is a dimensionless coefficient of the order of unity.

Of interest is to compare this relation to the growth rate of the beam-plasma instability in a smooth plasmaguide. Solving Eqs. (27) and (28) with $a(z) = \mathrm{const}$, one can easily obtain that

$$\gamma = M_2 \sqrt[3]{g_0 k_0 \omega_0}, \tag{40}$$

where ω_0 corresponds to the intersection of the beam line and one of the TG modes (1), i.e., $\omega_0 = k_0 u = \Omega_n(k_0)$

and M_2 is another dimensionless coefficient. Thus, the main modification introduced by the wall corrugation is the change in the instability regime — instead of the cubic root dependence of the growth rate (40) on the beam density, which is typical for a single-particle instability, we now have the square root (39), which is the token of a collective-type instability with the growth rate comparable to the frequency of beam oscillations. Evidently, the reason for this is the reduction of the beam-plasma interaction due to the singular nature of plasma modes. The obtained growth rate (39) corresponds to the beam crossing the singular plasma wave only twice over the period, while in a smooth plasmaguide it permanently interacts with the plasma.

This evaluation is valid if the growth rate (39) is much smaller than the plateau's width. In the opposite limit, when the beam-plasma resonance overlaps many mode-locked intervals and the growth rate (40) exceeds the largest plateau's width, the wall corrugation is negligible. As usual, the intermediate case causes many troubles and can hardly be studied analytically.

VI. CONCLUSION

The main result of this paper is the splitting of the entire spectrum of TG modes of a corrugated planar plasmaguide into different wave branches consisting of an infinity of subbands with constant rational wave numbers. This mode locking is usually thought of as an attribute of nonlinear physics but, amazingly, here we run it across in a linear problem.

Is the obtained spectrum dense? The devil's staircase does not form any dense set in the (κ, s) plane. If we rescale s to ω in, say, Fig. 3, cut and fold it along the ω axis to reduce it to the first Brillouin zone, then the resulting graph would not still constitute a dense set. To obtain something really dense, we should add an infinity of other graphs with rescaled κ corresponding to all $n \neq 1$. Therefore, whether this spectrum is to be called dense is a matter of definition and taste.

Nevertheless, the spectrum of TG modes in any closed planar resonator must be dense because of the reduced dimensionality of its geometric representation. For instance, the problem may be easily solved for a rectangular cavity, where the spectrum is given by Eq. (1) with k taking some discrete values. A less trivial example is a circle $x^2 + z^2 < 1$. Then, representing the solution of Eq. (4) in polar coordinates, ρ, θ, as $\phi = A(\rho\cos(\theta - \beta)) + B(\rho\cos(\theta + \beta))$, where $\cot\beta = s$, results in the functional equation $A(\cos(\theta - \beta)) + B(\cos(\theta + \beta)) = 0$. Expanding the latter in the Chebyshev polynomials, we get either $\sin(n\beta) = 0$ or $\cos(n\beta) = 0$, where n is an integer, which corresponds to the dense spectrum filling the band between zero and the plasma frequency.

To avoid confusion, it should be noted that many textbooks on partial differential equations state that there is no solution of hyperbolic-type equations like (4) in a closed area. The examples mentioned above correspond to the eigenvalue problem, which was seldom (if ever) discussed in the mathematical literature but is of physical sense.

There is still no answer to the question whether the discussed spectrum may appear in a cylindrical wave guide. One of the reasons for the mode locking is visible in Fig. 2: if two curves intersect at some point then because of the equidistance of the transverse wave numbers, q_n, in Eq. (1) there is an infinity of other curves coming through the same point. In a cylindrical waveguide q_n's are proportional to the roots of the Bessel functions, thus generally this property no longer holds. However, for large n the transverse wave numbers represent a nearly equidistant set and one may expect the mode locking to appear.

The presented theory of a corrugated plasmaguide is valid in a specific frequency band, $s > s_{\min}$, where the function $f(z, s)$ (9) is a circle map. An attempt to discard this limitation yields severe mathematical problems. When $s \to s_{\min}$, there appear confluent points of $f(z, s)$. In previously studied applications of circle maps (e.g., [6]), this bifurcation leads to the transition to chaos, which was, in fact, the main object of these studies. In the present context, if $s < s_{\min}$, then $f(z, s)$ becomes discontinuous, moreover, since the characteristic curve leaving the $x = 0$ axis can change the z direction of its propagation, $f(z, s)$ is no longer a circle map. It is associated with a flow at a more complicated manifold, like a sphere with two handles, and, to my knowledge, there is no detailed theory of corresponding maps.

Preliminary computer runs with $s < s_{\min}$ have shown that there is no (or, at least, little) chaos in characteristic curves and the spectrum remains qualitatively the same. This problem needs further investigation and will be discussed elsewhere.

Finally, as we have already mentioned, this theory has a number of over physical applications. For example, if Eq. (4) describes electromagnetic radiation in a resonator with oscillating walls, our results show that in a wide range of parameters a sequence of short pulses is formed. In other words, this may be considered as the Fermi acceleration of photons, which, in contrast with usual stochastic acceleration, is of regular character.

APPENDIX A: ARBITRARY CYCLES

The cycle points for an arbitrary plateau, $\Delta_{Q/P}$ are conveniently described by a function, $\sigma_{Q/P}$, which generalizes Eq. (16):

$$f^{(Q)}(z, \sigma_{Q/P}(z)) = \sigma_{Q/P}(z) + P. \tag{A1}$$

Obviously, $\sigma(z) = \sigma_{1/P}(z)$.

The following are some properties of $\sigma_{Q/P}(z)$ that may be easily derived from its definition.

(1) $\sigma_{Q/P}(z + 1) = \sigma_{Q/P}(z)$.

(2)There are exactly Q minima and Q maxima at the interval $[0, 1)$.

(3) All its extremal values are equal. The range of values of $\sigma_{Q/P}(z)$ is $\Delta_{Q/P}$.

(4) All cycle elements, $\alpha_n^{\pm}(s)$, are the roots of $\sigma_{Q/P}(z) = s$, so that $\sigma'_{Q/P}(\alpha_n^+) > 0$, $\sigma'_{Q/P}(\alpha_n^-) < 0$.

The general solution of Eq. (8) corresponding to $s \in$

$\Delta_{Q/P}$ and the wave number $k = \pi(2n + \lambda)Q/P$ is

$$A_z'^{\eta}(z,s) = \sum_{m=-\infty}^{\infty} \sum_{j=0}^{Q-1} e^{\pi i m(2n+\lambda)\frac{Q}{P}} (-1)^{\lambda j} \times \delta(z - \alpha_j^{\eta}(s) - m). \quad \text{(A2)}$$

The latter generalizes Eq. (20) and may be verified by straightforward substitution into Eq. (8).

Following the evaluation of Sec. III B, it is readily shown that the Stieltjes integral (24) with $A^{\eta}(z,s)$ given by Eq. (A2) represents a quasiperiodic function, such that

$$F(z+1) = e^{i\pi(2n+\lambda)Q/P} F(z). \quad \text{(A3)}$$

The whole z axis may be paved by alternating intervals $M_n^{\pm}$ with different signs of $\sigma'_{Q/P}(z)$. Since the values of $A(z,s)$ in different intervals are related by Eq. (8), the following constraint on $F(z)$ must hold:

$$F(g_{Q/P}(z)) = (-1)^{\lambda} F(z), \quad \text{(A4)}$$

where $g_{Q/P}(z) = f(z, \sigma_{Q/P}(z))$. Any function satisfying both relations (A3) and (A4) is determined by its value in any two adjacent intervals, say $M_0^{\pm}$, and therefore, may be represented as (24) with the inverse transform given by (25).

APPENDIX B: NUMERICAL METHODS

The computations where performed using the following algorithm.

1. Circle map

The circle map (9) is evaluated in few steps.

(1) The direction of a characteristic line (Fig. 1) is defined by a vector, $\mathbf{R}$, with $R_x = \pm s, R_z = \pm 1$. Starting from any point in (x,z) plane, a rough incremental search of the intersection between the line with a given $\mathbf{R}$ and the boundary $x = a(z)$ is performed. If the line goes down and crosses the z axis, the procedure is terminated.

(2) The coordinates of the intersection point, (x_0, z_0), are found by the Newton iteration method.

(3) The direction of propagation is chosen according to the value of $a'(z_0)$, which allows us to handle both simple paths depicted by the line 1 in Fig. 1 and more complicated situations (line 2). Then step (1) is recursively repeated.

The procedure is repeated to obtain any number of iterations of $f(z,s)$. The coordinates of all intersection points are stored, which allows us to use the recursion relation following from Eq. (9) to evaluate derivatives of $f^{(Q)}(z,s)$.

2. Devil's staircase

With $a(z)$ given by Eq. (18), plateaus with $Q = 1, 2$ were evaluated analytically. Equidistant values of s from the complementary set were taken ($\Delta s = 0.001$) to perform the rough search for cycles using a few hundred (usually 300) of map iterations for each s. The cycles with $Q > 100$ were discarded and, thus, some interval $(s_{\min}, s_{\max})$ was covered by first approximation plateaus.

This data was used for more exact computations. For all rational numbers Q/P ($Q < 100$, $Q/P < s_{\max}$), Eq. (A1) was solved by the Newton iteration method providing $\sigma_{Q/P}(z)$. The lower limit of Q/P was controlled by the condition $s > s_{\min}$. The iterations were initiated either by the position of the Q/P plateau already found during the rough search or, if no corresponding $\Delta_{Q/P}$ had been found yet, by the positions of nearby found plateaus. Finally, another iteration cycle was organized to locate the two adjacent extrema of $\sigma_{Q/P}(z)$ providing the edges of the plateau.

[1] W.R. Lou *et al.*, Phys. Rev. Lett. **67**, 2481 (1991).

[2] A.W. Trivelpiece and R.W. Gould, J. Appl. Phys. **30**, 1684 (1959).

[3] See, for example, J.M. Ziman, *Principles of the Theory of Solids* (Cambrige, University Press, 1972), Chap. 1.

[4] E.Z. Gusakov and A.D. Piliya, Pis'ma Zh. Eksp. Teor. Fiz. **48**, 71 (1988) [Sov. Phys. JETP Lett. **48**, 75 (1988)].

[5] See, for example, H.G. Schuster, *Deterministic Chaos* (Physik-Verlag, Weinheim, 1984).

[6] M.H. Jensen, P. Bak, and T. Bohr, Phys. Rev. A **30**, 1960 (1984).

[7] V.I. Arnol'd, *Geometrical Methods in the Theory of Ordinary Differential Equation* (Springer, Berlin, 1982).

[8] M.A. Lavrentiev and B.V. Shabat, *Problems in Hydrodynamics and Their Mathematical Models,* 2nd ed. (Nauka, Moscow, 1977).

[9] G.T. Moore, J. Math. Phys. **11**, 2679 (1970).

[10] V.V. Dodonov, A.B. Klimov, and V.I. Man'ko, *Proceedings of the P.N. Lebedev Physical Institute*, edited by M.A. Markov and V.I. Man'ko (Nauka, Moscow, 1992), Vol. 208, p. 105.

[11] B.B. Kadomtsev, *Collective Phenomena in Plasmas* (Nauka, Moscow, 1988).

[12] C.C. Lin, *The Theory of Hydrodynamic Stability* (Cambridge University Press, 1955).